

# Transport and interaction blockade of cold bosonic atoms in a triple-well potential

P. Schlagheck<sup>1,2</sup>, F. Malet<sup>1</sup>, J. C. Cremon<sup>1</sup>, and S. M. Reimann<sup>1</sup>

<sup>1</sup> Mathematical Physics, LTH, Lund University, Box 118, 22100 Lund, Sweden

<sup>2</sup> Département de Physique, Université de Liège, 4000 Liège, Belgium

## Abstract.

We theoretically investigate the transport properties of cold bosonic atoms in a quasi one-dimensional triple-well potential that consists of two large outer wells, which act as microscopic source and drain reservoirs, and a small inner well, which represents a quantum-dot-like scattering region. Bias and gate “voltages” introduce a time-dependent tilt of the triple-well configuration, and are used to shift the energetic level of the inner well with respect to the outer ones. By means of exact diagonalization considering a total number of six atoms in the triple-well potential, we find diamond-like structures for the occurrence of single-atom transport in the parameter space spanned by the bias and gate voltages. We discuss the analogy with Coulomb blockade in electronic quantum dots, and point out how one can infer the interaction energy in the central well from the distance between the diamonds.

PACS numbers: 67.85.-d, 03.75.Lm, 73.21.La

## 1. Introduction

The development of quasi one-dimensional waveguides for cold atoms based on optical lattices [1] and atom chips [2, 3] has led to a number of theoretical investigations on the guided quasi-stationary and dynamical transport properties of ultracold atomic gases [4–9]. Particular attention was devoted to the transport of coherent bosonic matter waves through quantum-dot potentials realized, e.g., by two (magnetic or optical) barriers along the waveguide, which display nonlinear transmission features that are reminiscent from nonlinear optics [6–10]. An important long-term aim in this context is to establish a close analogy with *electronic* conduction through microfabricated structures and nanostructures in solid-state systems. This latter field of research still exhibits a number of open questions especially related to the quantitative role of interaction and correlation between the electrons in such mesoscopic transport processes.

In spite of remarkable advancements in the creation of one-dimensional matter-wave beams through guided atom lasers [11, 12], the experimental realization and evaluation of such one-dimensional atomic scattering processes still represents a formidable task. It makes therefore sense to consider alternative approaches based on *closed* systems, where two reservoirs of ultracold atoms are connected to each other and biased such that a flow of atoms can take place from one reservoir to the other. Atomic quantum dots across which the atoms have to tunnel could be implemented by inducing small potential wells in between the reservoirs. Such geometries were studied in recent investigations on transistor-like operations with Bose-Einstein condensates [13]. The quantification of “conduction” across such a quantum dot under a small bias, however, requires a precise measurement of atomic populations ideally on a single-atom level, which is not impossible [14] but seems rather hard to be realized in this specific context.

A solution to the problem of counting individual atoms was recently provided by experiments with optical double-well lattices, focusing on correlated two-particle tunneling [15] as well as on the interaction blockade [16] with three particles [17]. In these experiments, each double-well site was identically prepared with a well-defined number of atoms and finally “read out” by absorption imaging after time-of-flight expansion, where the populations in the left and right wells were, before switching off the lattices, transferred to different Brillouin zones. This parallel processing of identical few-particle experiments especially allowed for the detection of integer atomic populations in each of the two wells per site [17], as a consequence of the strong repulsive interaction between the atoms. More recently, much theoretical work has focused on the tunneling of bosons in such double well potentials, see for example [18–22].

Inspired by the basic idea sketched above, we now propose here to investigate source-drain transport processes with ultracold atoms on the basis of optical *triple-well* lattices, which could possibly be realized by adding another standing-wave beam with the appropriate wavelength to the experimental setup in Refs. [15, 17]. If all three lattice potentials that together form the triple-well lattice are imposed with about the same amplitude and with a suitable phase shift relative to each other, a triple-well potential

can be created on each site where the two outer wells are considerably larger than the inner one. After loading the lattice with a well-defined number of atoms per site, these outer wells can be regarded as microscopic “source” and “drain” reservoirs, while the central well acts as an atomic quantum dot.

We now use this general configuration in this paper in order to study the atomic analog of *Coulomb blockade* in electron transport (see for example [23–27] and the review [28]) in the conduction of strongly interacting bosonic atoms from the source to the drain across the dot region. We consider, to this end, a time-dependent ramping process of a bias between the outer wells, which can be implemented by varying the amplitude and phase of the main (longest-wavelength) component of the triple-well lattice, and address the question to which extent this ramping process leads to the transfer of one or several atoms from the source reservoir to the dot or from there to the drain reservoir. While this perturbation represents the analog of a “bias voltage” in electronic quantum dots, a “gate voltage”, which lowers the on-site eigenenergies of the central well relative to the outer ones, can be induced in a very similar manner, again by a suitable manipulation of the main laser beam of the lattice. Our aim is to map out the lines of finite “conductance”, i.e. of a finite transfer of atoms between the wells, in the parameter space spanned by the above-mentioned gate and bias voltages. We shall show that this gives rise to diamond-like structures that are closely analogous to Coulomb diamonds in electronic quantum dots.

We start in Section 2 with a detailed description of the triple-well system under consideration, which is defined in accordance with the experimental setups used in Refs. [15,17]. Section 3 is devoted to the discussion of the “static” interaction blockade in the triple-well system in perfect analogy with the double-well interaction blockade experiment in Ref. [17]. In Section 4, we discuss the outcome of the time-dependent ramping process, which is numerically computed both through diagonalization of the many-body Hamiltonian as well as through the propagation of the many-body wavefunction under the variation of the bias. The resulting diamond structures are explained within a simple Bose-Hubbard model and compared with electronic Coulomb diamonds. We finally discuss the relevant energy scales of this transport process and point out possible implications for future research in the Conclusion.

## 2. The setup

We consider a gas of ultracold  $^{87}\text{Rb}$  atoms in a quasi one-dimensional confinement that is exposed to a periodic potential of the form

$$V(x) = V_0(-\cos kx + \cos 2kx - \cos 4kx) - V_g \cos kx - V_b \sin kx . \quad (1)$$

This potential can be generated by a superposition of three counter-propagating laser beams with the wavelengths  $\lambda_1 = \pi/k$ ,  $\lambda_2 = 2\pi/k$ , and  $\lambda_3 = 4\pi/k$ . We specifically consider the wavelengths  $\lambda_1 = 1530$  nm and  $\lambda_2 = 765$  nm, which were also used in the experiments of Refs. [15,17], and assume for the third laser beam the wavelength

$\lambda_3 = 382.5$  nm. The latter could possibly be realized by a frequency-doubling of the laser beam with the wavelength  $\lambda_2$  or, alternatively, by retro-reflecting a part of this laser beam (split with an acousto-optical deflector) under a finite angle of  $60^\circ$  as done in Ref. [29]. Using suitable phase shifts between these three counterpropagating laser beams (and taking into account the fact that the wavelength  $\lambda_1$  is red-detuned while the wavelengths  $\lambda_2, \lambda_3$  are blue-detuned with respect to the intra-atomic transition in  $^{87}\text{Rb}$ ), we thereby obtain the effective potential  $V_{\text{eff}}(x) = -2V_1 \cos^2(\frac{1}{2}kx - \phi/2) + 2V_2 \cos^2(kx) + 2V_3 \cos^2(2kx - \pi/2)$  with positive prefactors  $V_1, V_2$ , and  $V_3$ , which apart from a constant offset is exactly equivalent to Eq. (1) provided we choose  $V_1 \cos \phi = V_0 + V_g$ ,  $V_1 \sin \phi = V_b$ , and  $V_2 = V_3 = V_0$ . In this way, we obtain, as shown in Fig. 1, a periodic lattice of sites with triple-well potentials, where on each site the two outer wells are deeper than the central well.

The confinement to one spatial direction is assumed to be ensured by the presence of a strong two-dimensional (red-detuned) optical lattice in the transverse spatial directions, described by the effective potential  $V_{\text{tr}}(y, z) = -V_{\perp}(\cos k_{\perp}y + \cos k_{\perp}z)^2$ . This gives rise to a lattice of harmonic waveguides parallel to the  $x$ -axis with the confinement frequency  $\omega_{\perp} = 2k_{\perp}\sqrt{V_{\perp}/m}$  where  $m$  denotes the mass of a  $^{87}\text{Rb}$  atom. As was shown by Olshanii [30], the effective one-dimensional interaction strength along these waveguides is given by

$$g = \frac{2\hbar\omega_{\perp}a_s}{1 - Ca_s/a_{\perp}} \quad (2)$$

with  $C \simeq 1.4603$ , where  $a_s \simeq 5.8$  nm is the  $s$ -wave scattering length for  $^{87}\text{Rb}$  atoms and  $a_{\perp} \equiv \sqrt{\hbar/(m\omega_{\perp})}$  denotes the transverse oscillator length. Obviously, a rather large value for  $V_{\perp}$  is generally required in order to induce strong interactions along the one-dimensional confinement. Setting, as in the experiments of Refs. [15,17], the wavelength of the transverse laser beams to  $\lambda_{\perp} \equiv 2\pi/k_{\perp} = 843$  nm, we obtain the one-dimensional interaction strength  $g = 4\hbar^2k/m$  if we choose  $V_{\perp} = 690E_r^{\perp}$  with  $E_r^{\perp} \equiv \hbar^2k_{\perp}^2/(2m)$  being the transverse recoil energy.

We shall in the following consider also a large amplitude of the longitudinal triple-well lattice and set, for the sake of definiteness, the prefactor  $V_0$  in Eq. (1) to  $V_0 = 20\hbar^2k^2/m = 40E_r$  where  $E_r \equiv \hbar^2k^2/(2m)$  (corresponding to  $\simeq 7.8$  kHz) is the recoil energy of the laser with the wavelength  $\lambda_2$ . For this particular choice of the lattice strength, and for  $V_b = V_g = 0$ , the energetically lowest single-particle eigenstates within each triple-well site are strongly localized in the wells. A rather small splitting  $\delta E_{LR} \simeq 0.02\hbar^2k^2/m$  of the ground-state doublet, consisting of the positive and negative linear combination of the ‘‘Wannier states’’ (or quasi-modes) in which the atom is localized around the center of the left and right well, respectively, is thereby obtained, corresponding to a tunneling time scale of the order of  $\tau \sim \hbar/\delta E_{LR} \simeq 1$  ms. This splitting is much smaller than the level spacing between the ground-state doublet and the doublet containing an excited state in one of the wells, which is roughly characterized by the local harmonic-oscillator energy  $\hbar\omega_{\parallel} \simeq 4\hbar k\sqrt{V_0/m} \simeq 18\hbar^2k^2/m$  within the well. Tunneling between *adjacent* triple-well sites is neglected in the following, as

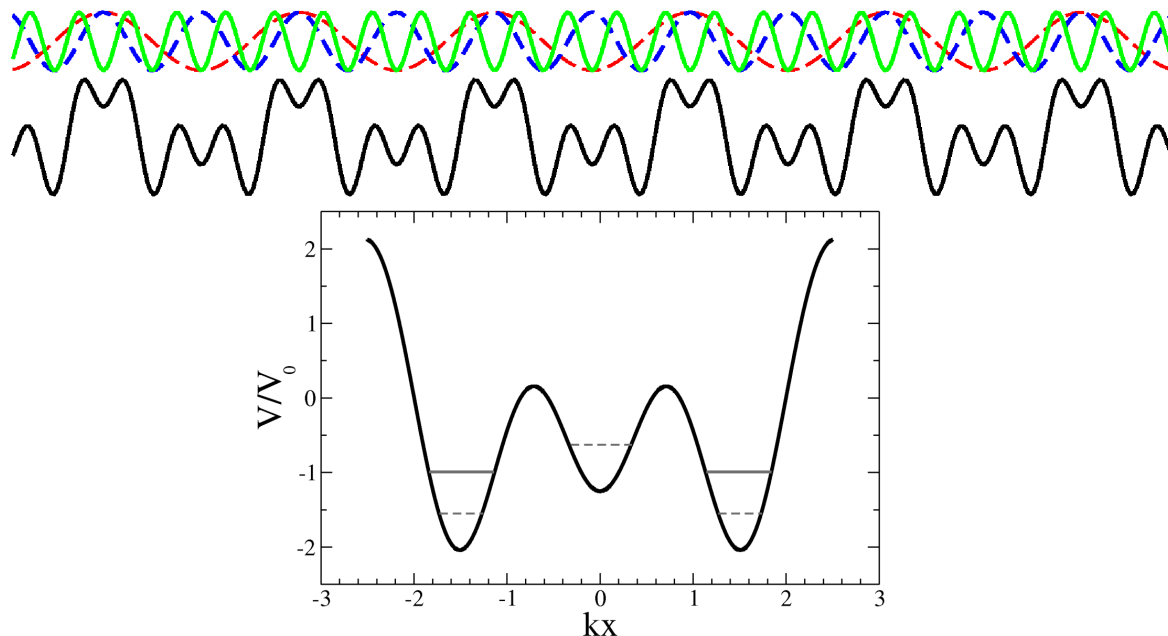


**Figure 1.** (color online) Three optical lattices with the commensurate periods  $2\pi/k$ ,  $4\pi/k$ , and  $8\pi/k$  (upper panel) are superimposed according to Eq. (1) to form a superlattice (middle panel). The lower panel displays the resulting triple-well potential on an individual site of the superlattice (for  $V_g = V_b = 0$ ). The dashed lines mark the unperturbed single-particle energies in the wells, and the solid lines indicate the chemical potential, or, more precisely, the particle-removal energy of an individual atom for the six-particle ground state where three atoms are localized in the left as well as in the right well.

the associated inter-site tunneling time exceeds all other relevant time scales of this system. We therefore consider the dynamics within the individual triple-well sites to be completely independent of each other.

In addition to the “main” triple-well lattice characterized by the amplitude  $V_0$ , we introduce in Eq. (1) two independent perturbations with the amplitudes  $V_g$  and  $V_b$  which can be controlled by a suitable manipulation of the laser beam with the largest wavelength  $\lambda_1$ . In close analogy with Coulomb blockade experiments in electronic quantum dots, we name  $V_g$  the “gate voltage” and  $V_b$  the “bias voltage”. Indeed, as for electronic quantum dots, the effect of increasing  $V_g$  is to lower the energetic offset of the central well with respect to the outer ones, which allows one to enhance the ground-state population of this well in the many-body system. A positive bias voltage  $V_b$ , on the other hand, gives rise to an overall tilt of the triple-well configuration, which opens the possibility for a transfer of individual atoms from the left to the central or from the central to the right well.

In lowest order, the impact of the gate and bias voltages  $V_g$  and  $V_b$  can approximately be quantified by the shifts  $E_L \rightarrow E_L + V_b$ ,  $E_C \rightarrow E_C - V_g$ , and  $E_R \rightarrow E_R - V_b$ , of the single-particle energies  $E_L$ ,  $E_C$ , and  $E_R$  in the left, central, and

right well, respectively. This result is obtained by a simple perturbative consideration where the matrix elements of the gate and bias perturbations in Eq. (1) are evaluated within the local ground states in the wells, which are approximated by Gaussian wavefunctions centred around  $kx = 0$  for the central and around  $kx = \pm\pi/2$  for the right and left well. Using  $\omega_{\parallel} \simeq 4k\sqrt{V_0/m}$  as local oscillator frequency and  $V_0 = 20\hbar^2k^2/m$ , we obtain  $E_{L/R} \rightarrow E_{L/R} \pm 0.986V_b$  and  $E_C \rightarrow E_C - 0.986V_g$ . This implies that the gate and bias “voltages” directly correspond here to the associated energy shifts in the individual wells.

### 3. Interaction blockade in the ground-state populations

As in Ref. [17], we assume that the superlattice is initially loaded with an ultracold gas of  $^{87}\text{Rb}$  atoms, such that each of the triple-well sites is populated with a given well-defined number of atoms. In the experiment of Ref. [17] which used a double-well lattice, interaction blockade was measured by detecting the ground-state populations in the left and right wells as a function of a finite bias between the wells. For this purpose, the population in the left well was transferred into a highly excited state within the double-well potential by means of a rather fast increase of the bias; this allows to separately detect it through time-of-flight expansion and subsequent absorption imaging after switching off the optical lattices (see also Ref. [15]). A step-like structure, with plateaus at integer values, was found for the population in the left and right wells as a function of the bias [17], which is a clear consequence of the strong repulsive interaction between the atoms.

This programme can be carried out as well for our triple-well configuration. Figure 2 shows, as a function of the bias voltage  $V_b$ , the populations in the left, central, and right well that is contained in the many-body ground state of six particles per triple-well site. As in Ref. [17], the populations undergo rather sharp, step-like transitions between plateaus at integer values, which clearly underlines the relevance of the strong repulsive interaction between the atoms. While the central well remains practically empty at the gate voltage  $V_g = 5$ , it is populated with one atom at  $V_g = 10$  provided the bias is not too strong. This scenario can straightforwardly be generalized to stronger gate voltages that would allow for two or more atoms in the central well. Decreasing the interaction strength will lead to a decrease of the bias voltage interval in which the sequence of transitions takes place, until in the limit of vanishing interaction this sequence shrinks down to a collective transition from a fully left-biased state, with all atoms in the left well, at negative to a fully right-biased state at positive bias voltages. An infinitely large interaction strength  $g$  will, on the other hand, not give rise to an infinite interaction energy within the wells and to an infinite extent of the plateaus, but rather approach the case of noninteracting spinless *fermionic* atoms [30] where the Pauli exclusion principle is responsible for the appearance of plateaus and step-like transitions in the populations.

The many-body ground states were calculated by means of an exact diagonalization approach based on the Lanczos algorithm [31], which takes into account all Fock states

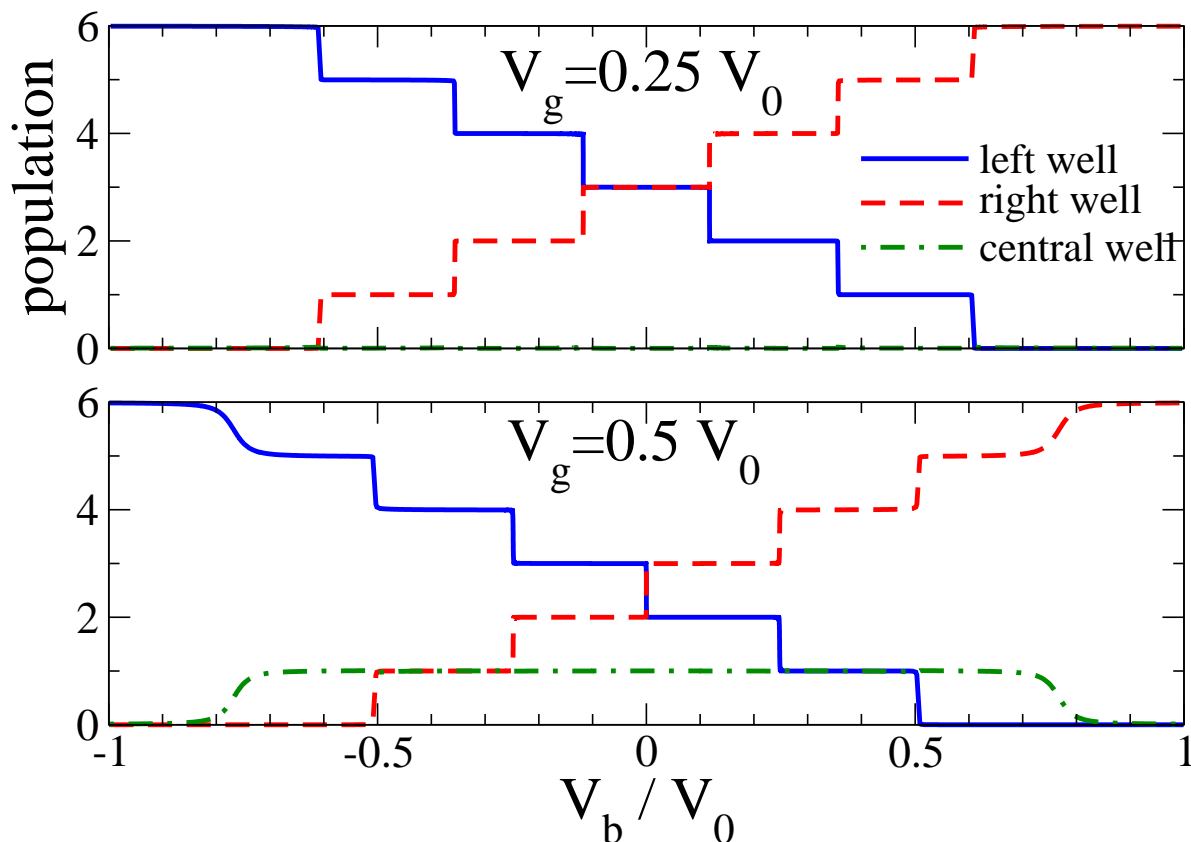


**Figure 2.** (color online) Populations in the left (solid blue line), right (dashed red line), and central well (dot-dashed green line) for the exact ground state of six particles in the triple-well potential as a function of the bias voltage  $V_b$ . The calculation was done for the gate voltages  $V_g = 0.25V_0$  (upper panel), for which the central well is practically empty, and for  $V_g = 0.5V_0$  (lower panel), for which the central well contains one atom at not too strong bias. Due to the strong repulsive interaction between the atoms, the populations in the wells undergo step-like transitions between plateaus at integer values under the variation of the potential, in close analogy with interaction blockade in double-well lattices [17].

with a given total number of particles that are defined upon a suitably truncated single-particle basis. We chose as basis functions the plane waves  $\phi_n(x) = \sqrt{k/(2\pi)}e^{inkx}$  that satisfy periodic boundary conditions within the triple-well lattice, and took into account for the many-body calculation all  $\phi_n$  with  $-10 \leq n \leq 10$ . We verified that for six particles this truncation is sufficient to reproduce all relevant features of the many-body states under consideration. After calculating the ground state and its many-body eigenfunction, the populations in the individual wells are computed by integrating the spatial atomic density in between (artificial) separation points at the local maxima of the triple-well potential. The population in the left well is thus obtained as the integral over the density from  $x = -\pi/k$  to the position of the left local maximum (at  $x \simeq -0.7/k$  for  $V_g = V_b = 0$ ), while the population in the central well is given by the integral over the density in between the left and right maxima.



With few exceptions (occurring notably at near-degeneracies between the energies of different many-body states), we almost always obtain nearly integer well populations for the eigenstates, due to the strong repulsive interaction between the atoms. We shall therefore denote these eigenstates by  $N_L:N_C:N_R$  in the following, where the integers  $N_L$ ,  $N_C$ , and  $N_R$  represent the populations in the left, central, and right well, respectively.

## 4. Interaction blockade in the transport

### 4.1. Time-dependent ramping process

In contrast to the double-well potential, the confinement (1) permits to probe interaction blockade not only in the “static” properties of the many-body ground state, but also in the dynamical *transport* behaviour of the system under the variation of the bias. We assume for this purpose that the triple-well lattice is initially loaded with a given number of atoms at a given gate voltage  $V_g$  and at vanishing bias  $V_b = 0$ . The bias voltage is then *dynamically ramped* from zero to a given maximal value on a suitable time scale. After this ramping process, the population in the individual wells is measured by a suitable transfer of the atoms to excited modes, time-of-flight expansion, and absorption imaging [15].

The speed of this ramping has to be chosen such that it is slow with respect to the tunneling time scale between adjacent wells (i.e., between the left and central well, or between the central and right well), but fast with respect to “direct” tunneling between the left and right well. More quantitatively, considering a linear ramping process of the form  $V_b(t) = st$  with constant speed  $s$ , and taking into account that the shift of the single-particle energy in the left or right well with respect to the central well is approximately given by  $V_b$  (as pointed out in Section 2), the Landau-Zener theory for nonadiabatic transitions [32] predicts the probability

$$P = 1 - \exp[-2\pi\Delta E^2/(\hbar s)] \quad (3)$$

for the transfer of an atom at an avoided crossing between the state  $N_L:N_C:N_R$  and the state  $N_L \pm 1:N_C \mp 1:N_R$  (or  $N_L:N_C \pm 1:N_R \mp 1$ ), where  $\Delta E$  denotes the level splitting between the hybridized states right at the anticrossing. If we denote by  $\delta E$  the analogous level splitting between  $N_L:N_C:N_R$  and  $N_L \pm 1:N_C:N_R \mp 1$ , corresponding to the transfer of an atom across both barriers, we obtain the requirement that the speed  $s$  of the ramping process would have to satisfy  $\delta E^2 \ll \hbar s < \Delta E^2$ .

In the spirit of this consideration, the outcome of this time-dependent ramping process can be predicted by computing not only the ground state, but also lowly excited states of the many-body system as a function of the bias voltage. The lower panel in Fig. 3 shows the result of such a numerical calculation, which was done for six particles at the gate voltage  $V_g = 0.25V_0$ . In accordance with Fig. 2, we recognize that the state with the populations 3:0:3, which is the energetically lowest state at zero bias, undergoes a small anticrossing with the 2:0:4 state at  $V_b \simeq 0.117V_0$ , which then represents the new ground state beyond that value of the bias voltage. The level splitting at this anticrossing



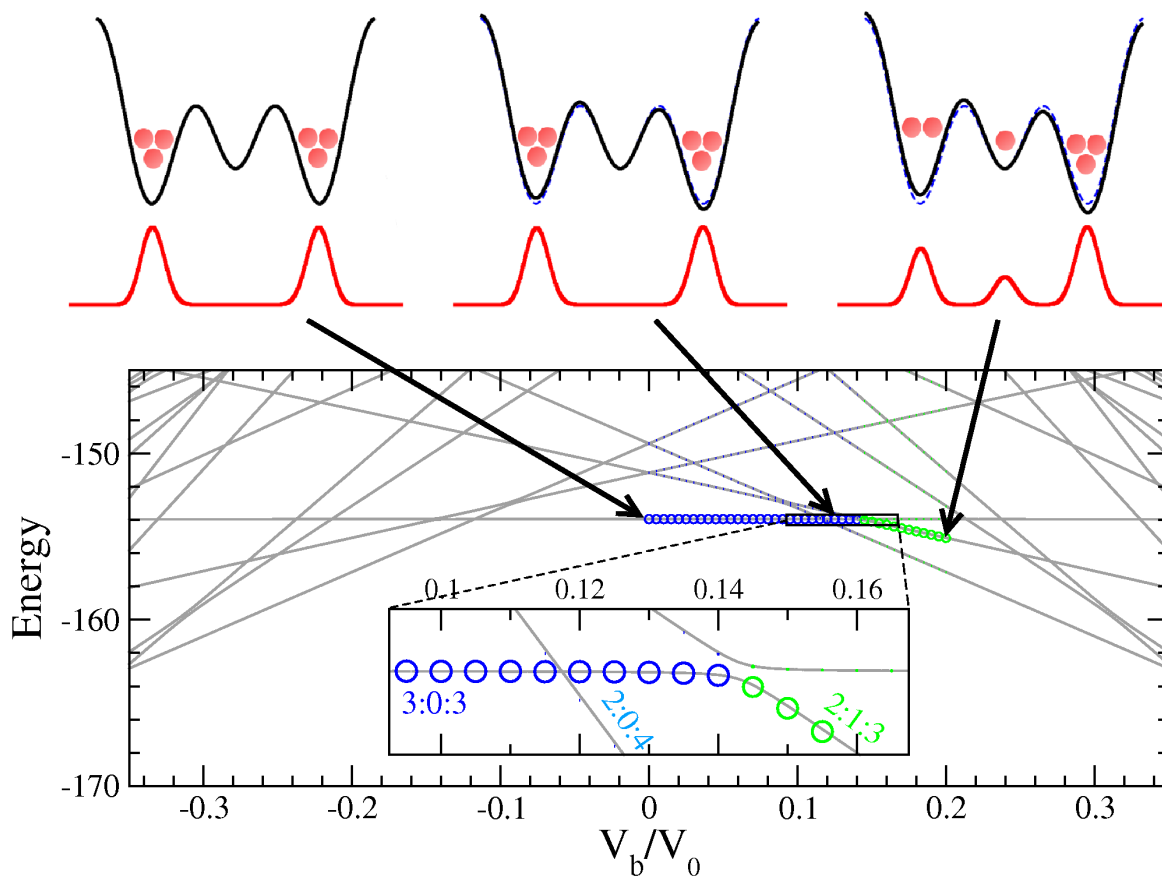


**Figure 3.** (color online) Time-dependent transport process for six particles in the triple-well potential. We start here from an unbiased configuration at gate voltage  $V_g = 0.25V_0$  (upper left panel), which is then exposed to a time-dependent sweep of the bias voltage from  $V_b = 0$  to  $V_b = 0.2V_0$  with the constant speed  $dV_b/dt = 0.002\hbar^3 k^4/m^2$ . The upper panels show the potential (above, in black) and the spatial atom densities (below, in red) for the bias voltages  $V_b = 0$  (left panel),  $V_b = 0.125V_0$  (middle panel), and  $V_b = 0.2V_0$  (right panel). The lower panel illustrates the evolution of this time-dependent ramping process in the many-body spectrum (energies are in units of  $\hbar^2 k^2/m$ ). We compute for this purpose the decomposition of the time-dependent many-body wavefunction into the instantaneous eigenstates of the Hamiltonian, and represent the relative weight of this decomposition by the size of the circles. Clearly, the system undergoes a nearly perfect transition from the 3:0:3 to the 2:1:3 state at the avoided crossing at  $V_b \simeq 0.143V_0$ , and is nearly not affected by the previous anticrossing between the 3:0:3 and 2:0:4 states at  $V_b \simeq 0.117V_0$ .

is found to be  $\delta E \simeq 0.001\hbar^2 k^2/m$ , which is much smaller than the subsequent splitting  $\Delta E \simeq 0.069\hbar^2 k^2/m$  between the levels of the 3:0:3 and the 2:1:3 states. Consequently, a ramping process  $V(t) = st$  with, e.g., the constant speed  $s = 0.002\hbar^3 k^4/m^2$ , altogether taking place within a time interval of  $\tau \simeq 0.2V_0/s \simeq 40$  ms, will provide the desired atom transfer from the left to the central well.

This is indeed confirmed by a truly time-dependent simulation of the ramping process. We use for this purpose a variant of the Lanczos algorithm [33], which involves

the creation of a finite Krylov subspace that contains the most relevant components describing the time derivative of the wavefunction to be propagated. Within short time intervals  $\delta t$ , a numerically precise propagation is carried out in this Krylov subspace, utilizing the representation of both the unperturbed part of the Hamiltonian and the time-dependent perturbation within this subspace [34]. In between those time intervals, the Krylov subspace is recreated using the “new” wavefunction that results from this propagation step. In practice, we find good convergence using 100 Krylov vectors and the time step  $\delta t = 1.0m/(\hbar k^2)$ .

The lower panel of Fig. 3 shows the result of such a time-dependent calculation for a ramping process of the bias voltage with the speed  $s = 0.002\hbar^3 k^4/m^2$  from  $V_b = 0$  to  $V_b = 0.2V_0$ . To illustrate the evolution in the many-body spectrum, we compute here at regular intervals in time the overlap matrix elements of the wavefunction with the instantaneous eigenstates of the Hamiltonian. This decomposition is then represented in Fig. 3 by circles whose sizes are directly proportional to the square moduli of those matrix elements. We basically see that the time-dependent wavefunction is, at almost all considered bias voltages, essentially described by one single eigenstate of the Hamiltonian, namely the one that exhibits the populations 3:0:3 before and 2:1:3 after the avoided crossing at  $V_b \simeq 0.143V_0$ . The small anticrossing between the 3:0:3 and the 2:0:4 states at  $V_b \simeq 0.117V_0$ , on the other hand, is almost completely “ignored” by the time-dependent wavefunction, which undergoes a *diabatic* transition across this anticrossing (in contrast to the adiabatic transition at  $V_b \simeq 0.143V_0$ ).

This calculation can be carried out for other gate voltages as well. Figure 4 shows, as a function of  $V_g$ , the minimal (positive and negative) bias voltages  $V_b$  until which the time-dependent ramping process has to be performed in order to obtain single-atom transfer between adjacent wells. The starting configuration depends on the gate voltage under consideration. For  $V_g < 0.4V_0$ , we start with a 3:0:3 population at zero bias, which is then transformed into a 2:1:3 state under the increase of  $V_b$ , and into a 3:1:2 state if instead the bias is ramped into the opposite direction leading to negative  $V_b$ . Within  $0.4V_0 < V_g < 0.72V_0$ , the initial state either corresponds to a 2:1:3 or to a 3:1:2 population, depending on the presence of a tiny positive or negative bias. The final state of the ramping process depends now on the gate voltage. For  $V_g < 0.56V_0$ , we obtain the 2:0:4 state (or the 4:0:2 state for negative bias), i.e. the atom in the central well is released to the right (left) well, while for  $V_g > 0.56V_0$  another atom from the left (right) well is pulled into the central well leading to the 1:2:3 (3:2:1) state. A completely analogous situation is realized for gate voltages within  $0.72V_0 < V_g < 1.28V_0$  where we initially encounter a 2:2:2 population — with the only exception that this population does obviously not depend on the presence of a small initial bias.

#### 4.2. Bose-Hubbard theory of the diamonds

The structure and shape of the transitions lines in the  $V_b$ - $V_g$  parameter space are strongly reminiscent of Coulomb diamonds in electronic quantum dots (see for example, the very

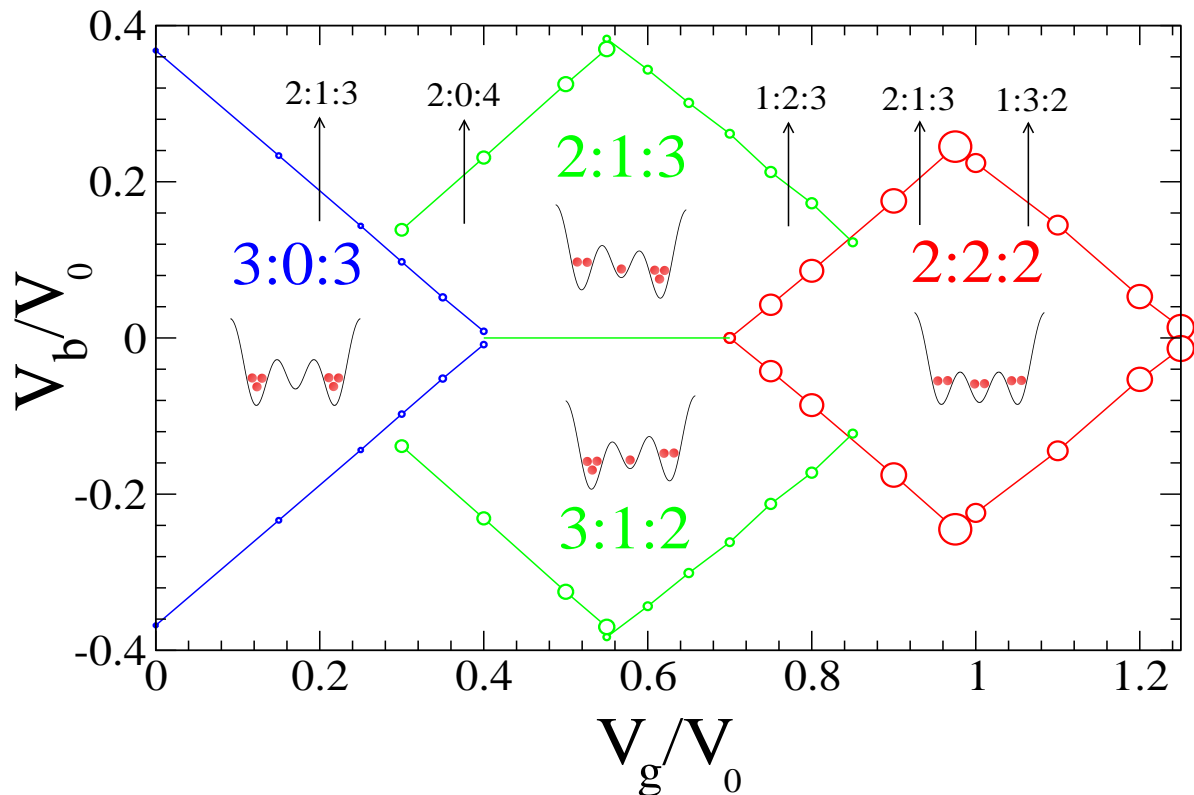


**Figure 4.** (color online) Interaction-blockade diamonds for six atoms in the triple-well potential. Plotted are the minimal (positive and negative) bias voltages  $V_b$  until which the time-dependent ramping process (symbolized by the vertical arrows) has to be performed in order to achieve single-atom transfer between adjacent wells. The circles mark the gate voltages for which numerical calculations, based on the computation of the many-body spectrum, were explicitly carried out. The size of the circles indicate the size  $\Delta V_b$  of the avoided crossings according to Eq. (21), which is proportional to their level splitting. Note that the avoided crossings become larger with larger  $V_g$ , which corresponds to the fact that the barrier height between the outer wells and the central well is lowered by increasing the gate voltage.

recent work of [35] or the review [28]). This analogy can indeed be straightforwardly worked out in terms of a simple Bose-Hubbard-type model. We take into account for this purpose the three energetically lowest single-particle eigenfunctions (or rather Wannier functions in the case of degeneracies)  $\phi_L(x)$ ,  $\phi_C(x)$ , and  $\phi_R(x)$ , corresponding to the particle being localized in the left, central, and right well. Approximating these single-particle eigenfunctions by normalized Gaussians centred around the minima of the  $(-\cos 4kx)$ -component of the potential, with a width that corresponds to the local oscillator length  $a_{\parallel} = \sqrt{\hbar/(m\omega_{\parallel})}$  with  $\omega_{\parallel} \simeq 4k\sqrt{V_0/m}$ , the shift of the corresponding single-particle energies due to the presence of finite gate and bias voltages is directly given by  $V_g$  and  $V_b$ , respectively. More precisely, these energies are approximately given by  $E_L = E_0 + V_b$ ,  $E_C = E_1 - V_g$ , and  $E_R = E_0 - V_b$ , with  $E_0 \equiv \langle \phi_{L/R} | H_0 | \phi_{L/R} \rangle$  and  $E_1 \equiv \langle \phi_C | H_0 | \phi_C \rangle$ , where we define  $H_0 \equiv -\frac{\hbar^2}{2m} \frac{\partial^2}{\partial x^2} + V_0(-\cos kx + \cos 2kx - \cos 4kx)$ .

The contact interaction  $U(x_1 - x_2) = g\delta(x_1 - x_2)$  gives rise to the local interaction

energies  $E_U^{(L/C/R)} = g \int |\phi_{L/C/R}(x)|^4 dx$  within each well. Using again the above Gaussian ansatz for the single-particle eigenfunctions, these interaction energies are approximately equal to each other and, for  $V_0 = 20\hbar^2 k^2/m$ , given by

$$E_U^{(L/C/R)} \simeq g \sqrt{\frac{m\omega_{||}}{2\pi\hbar}} \simeq 5.37 \frac{\hbar^2 k^2}{m} \simeq 0.268V_0 \equiv E_U. \quad (4)$$

Neglecting tunnel couplings between the wells, we obtain the Fock states  $|N_L, N_C, N_R\rangle$  built upon the single-particle basis  $(\phi_L, \phi_C, \phi_R)$  as eigenstates of the many-body system, where  $N_L, N_C, N_R$  represent the populations in the left, central, and right well, respectively. The corresponding eigenenergies read

$$E(N_L, N_C, N_R) = E_L(N_L) + E_C(N_C) + E_R(N_R) \quad (5)$$

with

$$E_L(N_L) = N_L (E_0 + V_b) + \frac{N_L(N_L - 1)}{2} E_U, \quad (6)$$

$$E_C(N_C) = N_C (E_1 - V_g) + \frac{N_C(N_C - 1)}{2} E_U, \quad (7)$$

$$E_R(N_R) = N_R (E_0 - V_b) + \frac{N_R(N_R - 1)}{2} E_U. \quad (8)$$

Tunneling across the barriers in the potential gives rise to hopping matrix elements between adjacent single-particle states which are, however, generally much smaller than the above energy scales. Their influence on the many-body eigenstates can therefore be neglected, except for accidental near-degeneracies between the unperturbed energies (5) where they give rise to hybridizations between the involved Fock states  $|N_L, N_C, N_R\rangle$ . The resulting avoided crossings in the many-body spectrum are most significant if the Fock states that participate at this crossing can be mapped into each other by the exchange of only one atom across one tunneling barrier.

In order to identify the location of these crossings in the parameter space spanned by the gate and bias voltages, we introduce the local particle-addition and -removal energies [16] as

$$\mu_{L/C/R}^+(N_{L/C/R}) \equiv E_{L/C/R}(N_{L/C/R} + 1) - E_{L/C/R}(N_{L/C/R}), \quad (9)$$

$$\begin{aligned} \mu_{L/C/R}^-(N_{L/C/R}) &\equiv E_{L/C/R}(N_{L/C/R}) - E_{L/C/R}(N_{L/C/R} - 1) \\ &= \mu_{L/C/R}^+(N_{L/C/R} - 1) \end{aligned} \quad (10)$$

for the left, central, and right well, respectively. With the help of Eqs. (6–8), we find

$$\mu_L^+(N_L) = E_0 + V_b + N_L E_U, \quad (11)$$

$$\mu_C^+(N_C) = E_1 - V_g + N_C E_U, \quad (12)$$

$$\mu_R^+(N_R) = E_0 - V_b + N_R E_U. \quad (13)$$

Degeneracies between unperturbed levels that correspond to the populations  $N_L:N_C:N_R$  and  $N_L \pm 1:N_C \mp 1:N_R$  therefore occur if  $\mu_L^\pm(N_L) = \mu_C^\mp(N_C)$ , which is equivalent to the equation

$$V_b = E_1 - E_0 - V_g + (N_C - N_L \mp 1)E_U. \quad (14)$$

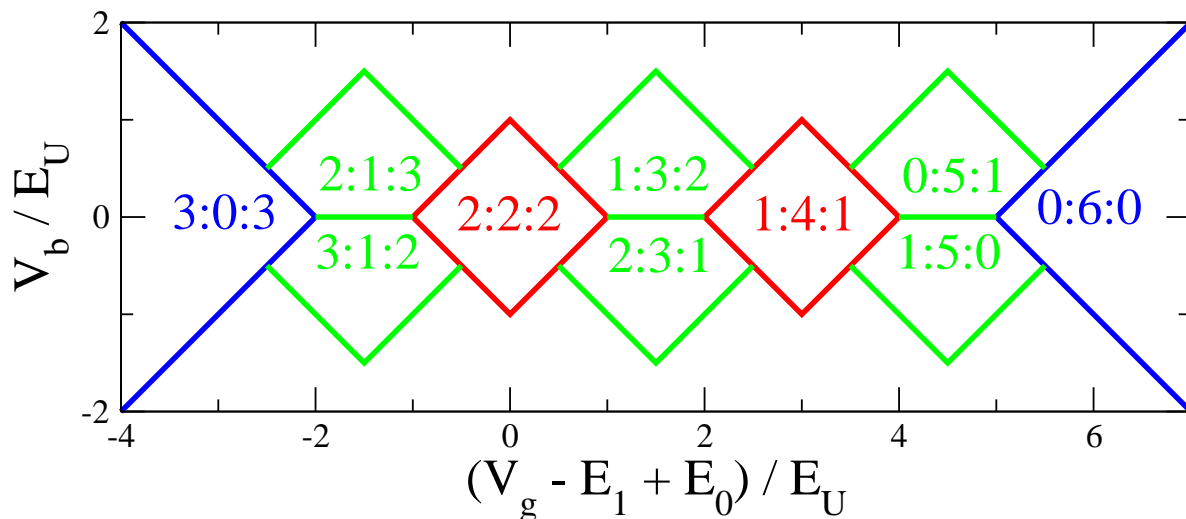


**Figure 5.** (color online) Structure of the interaction-blockade diamonds that result from a simple Bose-Hubbard-type model. Plotted are the predicted transition lines for single-particle transfer between adjacent wells according to Eqs. (14) and (15), assuming the presence of for six particles in a triple-well potential with equal on-site interaction energies. The agreement with Fig. 4 is rather good, taking into account the approximate value  $E_U \simeq 0.268V_0$  (4) for the interaction energy.

Correspondingly, we find

$$-V_b = E_1 - E_0 - V_g + (N_C - N_R \pm 1)E_U \quad (15)$$

as equation for the degeneracy between  $N_L:N_C:N_R$  and  $N_L:N_C \pm 1:N_R \mp 1$ .

With these equations (14) and (15), we can quantitatively predict the location and shape of the “atom blockade diamonds”, i.e. of the transition lines that mark the value of the bias at which single-atom transfer takes place between adjacent wells. This is shown in the Fig. 5 for the case of six particles in the triple-well potential under consideration. We see that the agreement with the numerically computed transition lines in Fig. 4 is rather good. Taking into account the approximate value (4) for the interaction energy  $E_U$ , we can quantitatively reproduce not only the shape, but also the size of the diamond structures in Fig. 4.

There are some important differences to standard Coulomb diamonds in quantum dots. On the one hand, the diamond structures display “open ends” both for very low and for very high gate voltages, corresponding to an empty quantum dot and to empty reservoirs, respectively. On the other hand, there is a significant asymmetry between the diamond structures corresponding to a “balanced” (with  $N_L = N_R$ ) and an “unbalanced” population (with  $N_L = N_R \pm 1$ ) in the outer wells. This is a consequence of the finite interaction energy  $E_U$  in the reservoirs.

To demonstrate this, we show in Fig. 6 a more mesoscopic situation involving 20 particles in total, where the two outer wells are assumed to be much more shallow and thereby exhibit a lower on-site interaction energy  $E_U^{(L/R)}$  than the central well. This

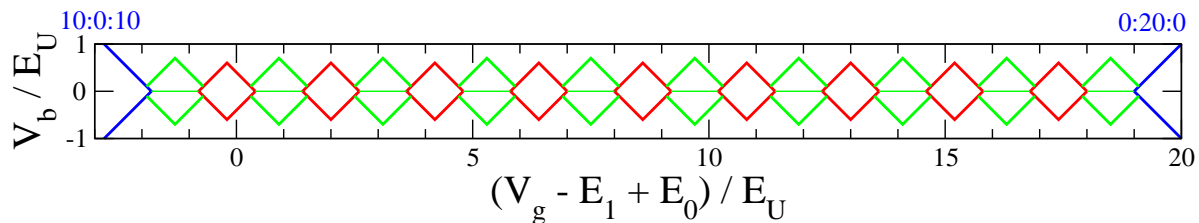


**Figure 6.** (color online) Same as Figure 5 for a more mesoscopic situation with 20 particles, where the two outer wells are assumed to be much more shallow and thereby exhibit a lower on-site interaction energy, namely  $E_U^{(L/R)} = 0.2E_U^{(C)} \equiv 0.2E_U$ , than the central well. This situation resembles much more the standard scenario of Coulomb blockade in electronic quantum dots where the two-particle interaction energy in the leads does not play a role.

leads to slight modifications of the formulas (14) and (15); we obtain

$$V_b = E_1 - E_0 - V_g + (N_C - 1)E_U^{(C)} - N_L E_U^{(L)}, \quad (16)$$

$$V_b = E_1 - E_0 - V_g + N_C E_U^{(C)} - (N_L - 1)E_U^{(L)}, \quad (17)$$

$$-V_b = E_1 - E_0 - V_g + (N_C - 1)E_U^{(C)} - N_R E_U^{(R)}, \quad (18)$$

$$-V_b = E_1 - E_0 - V_g + N_C E_U^{(C)} - (N_R - 1)E_U^{(R)}. \quad (19)$$

Specifically assuming  $E_U^{(L/R)} = 0.2E_U^{(C)}$  in Fig. 6, the resulting structure of the transition lines for single-particle transfer resembles much more the standard Coulomb diamonds in electronic quantum dots.

Independently of the size of the outer wells, the distance between the edges of the diamonds with balanced populations is, as seen from both in Fig. 5 and Fig. 6, predicted to be equal to the local interaction energy  $E_U^{(C)}$  in the central well. This opens the possibility to extract the value of this interaction energy from the location of the transition lines of single-atom transfer in the  $V_g$ - $V_b$  parameter space. From Fig. 4 we would approximately infer  $E_U^{(C)} \simeq 0.29V_0 \simeq 5.8\hbar^2k^2/m$  from the distance between the corners of the 3:0:3 and the 2:2:2 diamonds. This is in fairly good agreement with the numerically computed interaction energy  $E_U^{(C)} \simeq 5.1\hbar^2k^2/m$ , which is obtained by subtracting twice the lowest single-particle eigenenergy  $E_1$  of the central well from the energy of the lowest two-particle state where both electrons are localized in the central well.

### 4.3. Energy scales of the avoided crossings

While this simple Bose-Hubbard-type model is capable of reproducing the location of the transition lines for single-atom transfer in the  $V_g$ - $V_b$  parameter space, it is *not* sufficient to predict the time scales on which the ramping process ought to take place in order to achieve those transitions. As pointed out above, these time scales crucially depend on the sizes of the avoided crossings in the many-body spectrum, which are essentially given by the single-particle hopping matrix elements between different wells. These hopping matrix elements, however, arise from a tunneling process across the barriers

**Table 1.** Level splittings (in units of  $\hbar^2 k^2/m$ ) of the first two avoided crossings that are encountered during the ramping process of the bias voltage, for  $V_g = 0.25V_0$ ,  $0.5V_0$ , and  $1.0V_0$ .

gate voltage	initial state	first crossing			second crossing		
		bias voltage	crossing state	level splitting	bias voltage	crossing state	level splitting
$0.25V_0$	3:0:3	$0.117V_0$	2:0:4	0.0015	$0.143V_0$	2:1:3	0.069
$0.5V_0$	2:1:3	$0.248V_0$	1:1:4	0.019	$0.325V_0$	2:0:4	0.16
$1.0V_0$	2:2:2	$0.128V_0$	1:2:3	0.047	$0.221V_0$	1:3:2	0.22

that separate the wells from each other. They are therefore sensitively depending on the effective *height* of the barriers with respect to the particle-addition or -removal energies under consideration, which in turn is appreciably modified under variation of the bias or gate voltages.

Specifically, we find that an increase of the gate voltage, corresponding to “pulling down” the central well with respect to the outer ones, generally gives rise to a significant enlargement of the avoided crossings between different many-body levels. This is illustrated in Fig. 4 in which the size of the circles indicate the extent  $\Delta V_b$  of the avoided crossings between the states under consideration in bias voltage space. More precisely, if we describe the general dependence of the level splitting between two near-degenerate states on the bias voltage by

$$\Delta E(V_b) = \Delta E \sqrt{1 + \left( \nu(V_b - V_b^{(c)})/\Delta E \right)^2} \quad (20)$$

where  $\Delta E \equiv \Delta E(0)$  and  $V_b^{(c)}$  denote the splitting and bias voltage, respectively, at the crossing point and  $\nu$  represents the (nearly integer) difference between the variations of the unperturbed levels with  $V_b$  far away from the anticrossing. We define

$$\Delta V_b \equiv 2\Delta E/\nu \quad (21)$$

as the maximal extent of the avoided crossing in bias voltage space. For anticrossings that correspond to single-atom transfer between adjacent wells, we have  $\nu \simeq 1$  and therefore  $\Delta V_b \simeq 2\Delta E$ .

Table 1 lists the level splittings at the avoided crossings that the system undergoes during the time-dependent ramping process, for the gate voltages  $V_g = 0.25V_0$ ,  $0.5V_0$ , and  $1.0V_0$ . For each of those gate voltages, the first one of the encountered anticrossings corresponds to a double-barrier tunneling process of an atom which is directly transferred from the left to the right well. Correspondingly, the associated anticrossing is much smaller than the one of the second anticrossing describing a single-barrier tunneling process. This particularly implies that it is, for all of these cases, possible to define, according to the Landau-Zener formula (3), a reasonably large range of speeds  $s$  for the ramping process  $V_b(t) = st$ , such that the system undergoes a diabatic transition across the first and an adiabatic transition at the second anticrossing. Comparing, however, the level splittings for *different* values of  $V_g$ , we realize that this range of speeds will depend on the particular gate voltage under consideration, and that it is hardly possible



to choose one “universal” ramping speed with which the desired single-atom transfer can be carried out for all gate voltages. This is another specification of the microscopic nature of this transport system.

The size of the hopping matrix elements do also play a role for the question to which extent the interaction-blockade phenomena discussed here are also observable for lower effective one-dimensional interaction strengths  $g$ , i.e. in the presence of a weaker transverse confinement of the waveguide. Figure 5 seems to affirm this, as the structure of the diamonds does not explicitly depend on the interaction strength, except for the scaling of the horizontal and vertical axes which is directly proportional to  $g$ . However, the size and extent of the relevant avoided crossings, on the other hand, does, in lowest order, *not* scale with  $g$ , as they are essentially given by the single-particle hopping matrix element between adjacent sites. This implies that decreasing the effective interaction strength  $g$ , e.g., by a factor ten will, in lowest order, give rise to the same relative location of the transition lines in Fig. 4, with the  $V_g$  and  $V_b$  axes scaled down by a factor ten, while the “uncertainty” of the transition lines, given by the extent of the corresponding avoided crossings and represented by the size of the circles in Fig. 4, will be increased by a factor ten. The interaction-blockade diamonds ultimately become unobservable if the on-site interaction energy is of the same order as the tunneling matrix element between adjacent sites, in which case *collective* instead of single-atom transfer processes begin to take place. This underlines again the obvious requirement that the transport processes discussed here have to be performed in the “Mott-insulator regime” of strong on-site interaction and weak tunneling within the triple-well potential.

## 5. Discussion and conclusion

In summary, we studied a microscopic analog of source-drain transport with ultracold bosonic atoms in a triple-well potential. The latter is considered to be realized by optical triple-well lattices in analogy with the experiments of Refs. [15, 17], which are initially loaded with a well-defined number of atoms per site. We propose to perform then a time-dependent tilt of these triple-well potentials until a given maximal bias, followed by measuring the resulting populations in the individual wells. This process can be repeated for various values of a “gate voltage” which lowers the level of the central well with respect to the outer ones. Diamond structures are obtained for the transition lines that mark the necessary values for the bias in order to achieve single-atom transfer between adjacent wells, when being plotted as a function of that gate voltage. These diamonds can be used to infer the local interaction energy in the central well.

There are striking similarities with Coulomb diamonds in electronic quantum dots, but also some important differences to the latter, which mainly arise due to the microscopic nature of the “reservoirs” in the outer two wells. Most characteristically, “transport” is manifested not by a continuous flow of particles across the quantum dot, but rather by the transfer of a single atom from one well to another. This transport process is, in general, not “completed” insofar as the atom when, e.g., being transferred

from the left to the central well will not directly go on to the right well, due to the mismatch of the corresponding particle-addition and -removal energies. Close to the corners of the diamond structures (e.g. at  $V_g \simeq 0.3V_0$ , see Fig. 4), this latter task can eventually be achieved by further increasing the bias. In general, however, more complicated ramping processes, involving also a time-dependent variation of the gate voltage, would be required for that purpose. This is clearly a consequence of the finite two-body interaction energy in the reservoirs, which also leads to a striking asymmetry between diamond structures corresponding to balanced and unbalanced populations in the outer wells.

The microscopic transport scheme that we investigated here can be applied as well to more complex atomic gases involving, e.g., several spin components and/or long-range dipolar interaction. This will open various possibilities for the exploration of the interplay of interaction and transport in an experimentally feasible context. Our findings should, moreover, be relevant for cyclic processes [36] as well as for the evaluation of the feasibility of atomtronic scenarios and atomic transistors [13, 37, 38] and might provide valuable insight for the design of logical operations with single atoms.

## Acknowledgments

We would like to thank I. Bloch, I. Březinová, K. Capelle, G. Kavoulakis, M. Oberthaler, C. Pethick, M. Rontani, A. Wacker, and S. Zöllner for useful discussions. This work was financed by the Swedish Research Council and the Swedish Foundation for Strategic Research. The collaboration is part of the NordForsk Nordic network *Coherent Quantum Gases - From Cold Atoms to Condensed Matter*

## References

- [1] O. Morsch and M. Oberthaler, *Rev. Mod. Phys.* **78**, 179 (2006).
- [2] R. Folman, P. Krüger, D. Cassettari, B. Hessmo, T. Maier, and J. Schmiedmayer, *Phys. Rev. Lett.* **84**, 4749 (2000).
- [3] J. Fortágh and C. Zimmermann, *Rev. Mod. Phys.* **79**, 235 (2007).
- [4] P. Leboeuf and N. Pavloff, *Phys. Rev. A* **64**, 033602 (2001).
- [5] P. Leboeuf, N. Pavloff, and S. Sinha, *Phys. Rev. A* **68**, 063608 (2003).
- [6] I. Carusotto and G. C. La Rocca, *Phys. Rev. Lett.* **84**, 399 (2000).
- [7] I. Carusotto, *Phys. Rev. A* **63**, 023610 (2001).
- [8] T. Paul, K. Richter, and P. Schlagheck, *Phys. Rev. Lett.* **94**, 020404 (2005).
- [9] T. Paul, M. Hartung, K. Richter, and P. Schlagheck, *Phys. Rev. A* **76**, 063605 (2007).
- [10] K. Rapedius, D. Witthaut, and H. J. Korsch, *Phys. Rev. A* **73**, 033608 (2006).
- [11] W. Guerin, J.-F. Riou, J. P. Gaebler, V. Josse, P. Bouyer, and A. Aspect, *Phys. Rev. Lett.* **97**, 200402 (2006).
- [12] A. Couvert, M. Jeppesen, T. Kawalec, G. Reinaudi, R. Mathevet, and D. Guéry-Odelin, *EPL* **83**, 50001 (2008).
- [13] J. A. Stickney, D. Z. Anderson, and A. A. Zozulya, *Phys. Rev. A* **75**, 013608 (2007).
- [14] T. Campey, C. J. Vale, M. J. Davis, N. R. Heckenberg, H. Rubinsztein-Dunlop, S. Kraft, C. Zimmermann, and J. Fortágh, *Phys. Rev. A* **74**, 043612 (2006).

- [15] S. Fölling, S. Trotzky, P. Cheinet, M. Feld, R. Saers, A. Widera, T. Müller, and I. Bloch, *Nature* **448**, 1029 (2007).
- [16] K. Capelle, M. Borgh, K. Kärkkäinen, and S. M. Reimann, *Phys. Rev. Lett.* **99**, 010402 (2007).
- [17] P. Cheinet, S. Trotzky, M. Feld, U. Schnorrberger, M. Moreno-Cardoner, S. Fölling, and I. Bloch, *Phys. Rev. Lett.* **101**, 090404 (2008).
- [18] D.R. Dounas-Frazer, A.M. Hermundstad, and L.D. Carr, *Phys. Rev. Lett.* **99**, 200402 (2007).
- [19] S. Zöllner, H.D. Meyer, and P. Schmelcher, *Phys. Rev. A* **75**, 043608 (2007).
- [20] S. Zöllner, H.P. Meyer, and P. Schmelcher, *Phys. Rev. A* **78**, 013621 (2008).
- [21] S. Zöllner, H.D. Meyer, and P. Schmelcher, *Phys. Rev. Lett.* **100**, 040401 (2008).
- [22] D.V. Averin, T. Bergeman, P.R. Hosur and C. Bruder, *Phys. Rev. A* **78**, 031601 (2008).
- [23] J. Lambe and R. C. Jaklevic, *Phys. Rev. Lett.* **22**, 1371 (1969).
- [24] D.V. Averin and K.K. Likharev, *J. Low Temp. Phys.* **62**, 345 (1996).
- [25] D.V. Averin, and K.K. Likharev, in *Mesoscopic Phenomena in Solids*, B.I. Altshuler, P.A. Lee, and R.A. Webb, eds., Elsevier, Amsterdam (1991).
- [26] H. Grabert, and M.H. Devoret, eds., *Single Charge Tunneling*, Plenum Press, New York (1991).
- [27] Y. Meir, N.S. Wingreen, and P.A. Lee, *Phys. Rev. Lett.* **66**, 3048 (1991).
- [28] S. M. Reimann and M. Manninen, *Rev. Mod. Phys.* **74**, 1283 (2002).
- [29] E. Kierig, U. Schnorrberger, A. Schietinger, J. Tomkovic, and M. K. Oberthaler, *Phys. Rev. Lett.* **100**, 190405 (2008).
- [30] M. Olshanii, *Phys. Rev. Lett.* **81**, 938 (1998).
- [31] C. Lanczos, *J. Res. Natl. Bur. Stand.* **45**, 255 (1950).
- [32] C. Zener, *Proc. R. Soc. London A* **137**, 696 (1932).
- [33] T. J. Park and J. C. Light, *J. Chem. Phys.* **85**, 5870 (1986).
- [34] We subdivide for this purpose the time interval  $\delta t$  into 10000 sub-intervals within which we assume the Hamiltonian to be locally time-independent. The propagation within such a sub-interval is performed by explicit matrix exponentiation.
- [35] A. Fuhrer, L.E. Fröberg, J.N. Pedersen, M.W. Larsson, A. Wacker, M.-E. Pistol, and L. Samuelson, *Nano Letters* **7**, 243 (2007)
- [36] M. Hiller, T. Kottos, and D. Cohen, *EPL* **82**, 40006 (2008).
- [37] B. T. Seaman, M. Krämer, D. Z. Anderson, and M. J. Holland, *Phys. Rev. A* **75**, 023615 (2007).
- [38] R. A. Pepino, J. Cooper, D. Z. Anderson, and M. J. Holland, *Phys. Rev. Lett.* **103**, 140405 (2009).